

# Performance Analysis of Maximum Eigenvalue Detection in Nakagami- $m$ and Rice Fading Channels

Ricardo A. da S. Júnior  
National Institute of  
Telecommunications - Inatel  
P.O. Box 05 - 37540-000  
Santa Rita do Sapucaí - MG - Brazil  
ricardojunior@inatel.br

Rausley A. A. de Souza  
National Institute of  
Telecommunications - Inatel  
P.O. Box 05 - 37540-000  
Santa Rita do Sapucaí - MG - Brazil  
rausley@inatel.br

Dayan A. Guimarães  
National Institute of  
Telecommunications - Inatel  
P.O. Box 05 - 37540-000  
Santa Rita do Sapucaí - MG - Brazil  
dayan@inatel.br

**Abstract**— The aim of this paper is to present a performance analysis of the maximum eigenvalue detection (MED) for centralized data-fusion cooperative spectrum sensing in cognitive radio networks over Nakagami- $m$  and Rice fading channels. In the case of Nakagami- $m$ , arbitrary fading and phase parameters were assumed, and so was the case with Rice parameter of the Rician model.

**Index Terms**— cognitive radio, cooperative eigenvalue spectrum sensing, Nakagami, Rice.

## I. INTRODUCTION

In the context of fast developing wireless communications systems and consequent challenges, there is a growing need for effective use of spectrum and spectral efficient management strategies. The spectrum resources have become increasingly scarce, and at the same time there is a growing demand for better quality of service, as well as higher transmission rates. Nevertheless, there is in fact an artificial scarcity of spectrum, since there are bands that are not actually used during all time in a given region [1]. The cognitive radio (CR) technology [2], which aims at using the electromagnetic spectrum more efficiently, can be applied to this context. The CR system uses advanced techniques that optimize the occupation of the bands, and spectrum sensing techniques to find the so-called spectral opportunities within bands of interest in a given area and in a given time. Thus, the CR system makes it possible to use spectrum in temporal, spatial and frequency dimensions, without causing interference to licensed systems. Nonetheless, the scenarios of spectral occupancy differ depending on several factors, such as channel conditions, location and prevailing political control of spectrum usage. This implies greater system complexity, since the cognitive cycle of the CR concept includes a step for learning the channel [2][3]. Thus, the behavior of the channel influences the operation of the CR and, therefore, its performance. Then, evaluating the performance of a CR system in under different channel models is of paramount importance. In addition, each spectrum sensing technique will influence the detection performance, depending on the cognitive network architecture and the conditions of the channel. Many detection techniques for spectrum sensing have been proposed so far, e.g. the matched filter, the

cyclostationary and the energy detection [4][5]. Among the latest ones are those based on the eigenvalues of the received signal covariance matrix [6]-[8].

No matter the sensing technique adopted, the detection performance depends on the reception conditions of the CRs, and therefore on the propagation environment. For example, in [9] comparisons were made among different models for the energy detector under conditions of additive white Gaussian noise (AWGN) and Rayleigh fading channels. It has been verified that the problem of energy detection lies in the uncertainty of estimating the noise power, which degrades the detection performance [10]-[12]. In [13] the authors analyze the probability of miss detection of the energy detector under Nakagami fading channels.

This paper aims at presenting the analysis of the spectrum sensing performance under two important channel models: Nakagami- $m$  [14] (with arbitrary fading parameter) and Rice [15] (with Rice arbitrary parameter). The Nakagami distribution can be parameterized to model various fading conditions such as Rayleigh and Rice. This means that it is possible to control the severity of the Nakagami fading by making this distribution to fit more appropriately into real scenarios with multipath propagation [13]. The Nakagami- $m$  and Rice distributions, which are general, flexible, and mathematically easily tractable, have also been proved useful in practice [16]-[17]. In what concerns the detection technique, we consider the maximum eigenvalue detection (MED), also known as RLRT (Roy's largest root test) [7] or BCED (blindly combined energy detection) [6], applied to a centralized data-fusion cooperative spectrum sensing scheme.

The remainder of this paper is structured as follows. Section II presents the system model for the eigenvalue-based sensing technique and the fading channels models. Section III reports simulation results and discussions concerning the influence of some system parameters on the spectrum sensing performance. Finally, Section IV presents the conclusions.

## II. SYSTEM MODEL

### A. Centralized Cooperative Eigenvalue Spectrum Sensing

Although sensing can be performed by each secondary receiver in a non-cooperative fashion, cooperative spectrum sensing is considered a possible solution for problems

experienced by CR networks in a non-cooperative sensing situation, like receiver uncertainty, multipath fading, hidden terminals and correlated shadowing [3].

In what concerns the baseband memoryless linear discrete-time MIMO fading channel model, it is assumed here that there are  $\ell$  single-antenna CRs, each one collecting  $n$  samples of the received signal from  $k$  primary transmitters during the sensing period, and that these samples are arranged in a matrix  $\mathbf{Y} \in \mathbb{C}^{\ell \times n}$ . Similarly, consider that the signal samples transmitted from the  $k$  primary transmitters are arranged in a matrix  $\mathbf{X} \in \mathbb{C}^{k \times n}$ , and that  $\mathbf{H} \in \mathbb{C}^{\ell \times k}$  is the channel matrix with elements  $\{h_{ij}\}$ ,  $i = 1, 2, \dots, \ell$  and  $j = 1, 2, \dots, k$ , representing the channel gain between the  $j$ -th primary transmitter and the  $i$ -th CR receiver. In the present model, the elements in the channel matrix  $\mathbf{H}$  simulate a flat Nakagami- $m$  or Rice fading channel between each primary transmitter and CR, assumed to be constant during a sensing period and independent from one period to another (see subsections II.C and II.D). Finally, if  $\mathbf{V} \in \mathbb{C}^{\ell \times n}$  represents the matrix containing thermal noise samples that corrupt the received signal, then the matrix of collected samples is

$$\mathbf{Y} = \mathbf{H}\mathbf{X} + \mathbf{V}. \quad (1)$$

In eigenvalue-based spectrum sensing, spectral holes are detected by using test statistics based on the eigenvalues of the received signal sample covariance matrix. In a centralized cooperative scheme with data-fusion, matrix  $\mathbf{Y}$  is formed at the fusion center (FC), and the sample covariance matrix

$$\mathbf{R} \cong \frac{1}{n} \mathbf{Y}\mathbf{Y}^\dagger \quad (2)$$

is estimated, where  $(\cdot)^\dagger$  stands for complex conjugate and transpose. The maximum eigenvalue  $\lambda_1$  of  $\mathbf{R}$  is then computed and, assuming a single primary transmitter ( $k = 1$ ), the test statistic for MED is computed according to [7]:

$$T_{\text{MED}} = \frac{\lambda_1}{\sigma^2}, \quad (3)$$

where  $\sigma^2$  is the thermal noise power, which is assumed to be known.

### B. Binary Hypothesis Test in Spectrum Sensing

Spectrum sensing can be formulated as a binary hypothesis test problem, i.e.

$$\begin{aligned} \mathcal{H}_0 &: \text{Primary signal is absent} \\ \mathcal{H}_1 &: \text{Primary signal is present,} \end{aligned} \quad (4)$$

where  $\mathcal{H}_0$  is the null hypothesis, meaning that there is no licensed user signal active in a specific band, and  $\mathcal{H}_1$  is the alternative hypothesis, which indicates that there is an active primary user signal.

Two important parameters associated with the assessment of the spectrum sensing performance are the probability of detection,  $P_D$ , and the probability of false alarm,  $P_{FA}$ , which are defined as follows:

$$\begin{aligned} P_D &= \Pr\{\text{decision} = \mathcal{H}_1 | \mathcal{H}_1\} = \Pr\{T_{\text{MED}} > \gamma | \mathcal{H}_1\} \\ P_{FA} &= \Pr\{\text{decision} = \mathcal{H}_1 | \mathcal{H}_0\} = \Pr\{T_{\text{MED}} > \gamma | \mathcal{H}_0\}, \end{aligned} \quad (5)$$

where  $\Pr\{\cdot\}$  is the probability of a given event,  $T_{\text{MED}}$  the MED test statistic and  $\gamma$  the decision threshold. The value of  $\gamma$  is chosen depending on the requirements for the spectrum sensing performance, which are typically evaluated through receiver operating characteristic (ROC) curves that show  $P_D$  versus  $P_{FA}$  as they vary with the decision threshold  $\gamma$ .

### C. Nakagami- $m$ Fading Channel

In [18], the Nakagami channel modeling is discussed considering the statistics of the phase distribution of the channel, besides the envelope distribution, which continues to be a debatable question. Such distributions, including others as Rayleigh, typically model the envelope of the received signal assuming that the phase distribution is uniform, which is not generally true in real channels. The knowledge of the statistics applied to the phase distribution are important to communication systems analysis, for example when deriving the error probability of digital modulation schemes over fading channels, or when designing or analyzing the performance of carrier-tracking loops. Likewise, the phase distribution is important for analyzing the performance of spectrum sensing schemes, since it will affect the channel between primary transmitters and secondary receivers, as can be easily inferred from Subsection II.A.

Characterization and modeling Nakagami communication channels have been the focus of many researchers, because the Nakagami process models numerous classes and fading channel conditions, resulting in a model that fits empirical data more accurately [13]-[19]. Moreover, the Nakagami- $m$  distribution is mathematically simple, facilitating mathematical derivations, and thus making it more attractive for performance analysis. Besides, it brings flexibility and control in the severity of fading, taking for example the case of the Rayleigh fading as a particular situation.

As is well known, a Nakagami- $m$  variate can be obtained as the square root of a Gamma variate, which, in turn, is given by the sum of  $2m$  squared independent zero mean Gaussian variables. The parameter  $m$  is known as the Nakagami fading factor and it is used to control the severity of the fading channel. According to [18]-[20], the model for generating a complex Nakagami variate is based on the in-phase and quadrature probability density functions (pdf) of the corresponding fading process, which are respectively given by

$$f_x(x) = \left(\frac{m}{\Omega}\right)^{\frac{1+p}{2}m} \frac{|x|^{(1+p)m-1} \exp\left(-\frac{m x^2}{\Omega}\right)}{\Gamma\left(\frac{1+p}{2}m\right)} \quad (6)$$

$$f_y(y) = \left(\frac{m}{\Omega}\right)^{\frac{1+p}{2}m} \frac{|y|^{(1+p)m-1} \exp\left(-\frac{m y^2}{\Omega}\right)}{\Gamma\left(\frac{1+p}{2}m\right)}. \quad (7)$$

with  $-\infty < x < \infty$  and  $-\infty < y < \infty$ .

In the above densities, the second moment of the resulting fading envelope fluctuations is represented by  $\Omega$ . The parameter  $p$ , termed the Nakagami phase factor, is the condition of balance or unbalance between the in-phase and quadrature components of the fading process [18], which corresponds to the balance or unbalance between the real and imaginary components of the complex Nakagami random variate. Thus, in a more general scenario, one can think of an unbalanced structure between components, but still having a total of  $2m$  Gaussian processes. The value of  $p$  can be selected from  $-1 \leq p \leq 1$ , with the condition that  $p = 0$  leads to the balancing of the generation model, i.e. the same number of real and imaginary Gaussian variates. As shown in [18], this condition enables the correct distribution of the envelope and phase of the Nakagami fading process. This means that it is possible to evaluate the performance of the spectrum sensing more appropriately by using this Nakagami fading model.

Here, the real and imaginary parts of the complex Nakagami random variate were generated by using the inverse cumulative distribution function (or, simply, inverse cdf) method [21]. The goal was to simulate channel gains that follow the Nakagami distribution with unitary second moment (unitary average gain). This criterion must be met in order to achieve the correct signal-to-noise ratio (SNR) for the simulations, without any channel gain calibration.

The validation of the Nakagami channel modeling was performed by comparing the estimated pdfs of the envelope and phase of the complex Nakagami random variable with the theoretical ones, which are respectively given by

$$f_R(r) = \frac{2m^m r^{2m-1}}{\Omega^m \Gamma(m)} \exp\left(-\frac{mr^2}{\Omega}\right), r \geq 0, \quad (8)$$

$$f_\theta(\theta) = \frac{\Gamma(m)}{2^m \Gamma\left(\frac{1+p}{2}m\right) \Gamma\left(\frac{1-p}{2}m\right)} \frac{|\sin 2\theta|^{m-1}}{|\tan 2\theta|^{pm}}, -\pi < \theta \leq \pi. \quad (9)$$

Figure 1 shows the estimated and theoretical densities for the Nakagami envelope, assuming  $\Omega = 1$ . In this figure, as well as in Figures 2, 3 and 4, the solid lines correspond to the theoretical results, whereas the dots are associated with the generated random variates. One can notice the close agreement between experimental and theoretical densities.

Besides validating the envelope fluctuations, it is necessary to examine the theoretical and estimated phase distributions of the generated complex Nakagami variate. Figure 2 shows results for the phase densities considering different values of the fading factor  $m$ . Notice that, as expected, the pdf of the phase component follows a uniform distribution for the case where the fading factor leads to a Rayleigh fading ( $m = 1$ ). It is worth mentioning that the generation model adopted here includes non-integer values for the  $m$  factor and that the phase factor  $p$  must be equal to zero to produce a balanced complex Nakagami random variate.

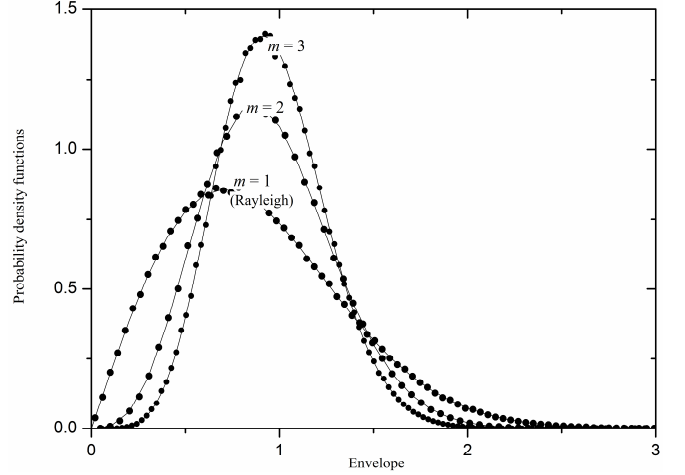


Fig. 1. Empirical and theoretical Nakagami- $m$  envelope densities

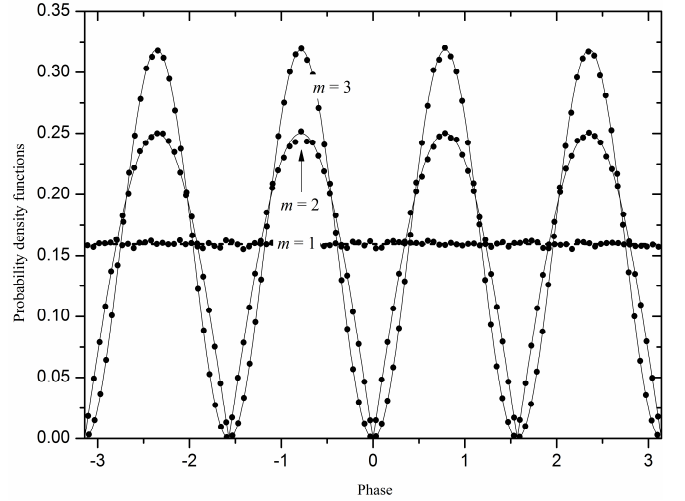


Fig. 2. Empirical and theoretical Nakagami- $m$  phase densities under  $m$  parameter variations

#### D. Rice Fading Channel

In the Rice fading channel model, fading severity is governed by the Rice factor, which is the ratio between the powers of the dominant received signal component (referred to  $A^2$ ) and those produced by the multipath propagation (referred to  $2\sigma^2$ ). The higher this ratio, the less severe are the effects of the fading because of the presence of a line-of-sight (LOS) or a dominant multipath component signal. For example, the channel in a cognitive radio system having a LOS with a primary transmitter can be modeled with multiple cases of the Rice fading. So, it is in order to assess the performance of the spectrum sensing process in Rice fading channels. More specifically, it would be interesting to see how the detection performance is impacted by the variation of the Rice factor.

The model adopted here for generating a complex Ricean variate was based on the corresponding magnitude and phase pdfs of the fading process, which are respectively given by

$$f_R(r) = \frac{r}{\sigma^2} \exp\left(-\frac{r^2 - A^2}{2\sigma^2}\right) I_0\left(\frac{rA}{\sigma^2}\right), r \geq 0, A \geq 0 \quad (10)$$

$$f_{\Theta}(\theta) = \frac{1}{2\pi} e^{-K} \times \left\{ 1 + \sqrt{4\pi K} e^{K \cos^2 \theta} \cos \theta [1 - Q(\sqrt{2K} \cos \theta)] \right\}, \quad (11)$$

where  $-\pi < \theta \leq \pi$ ,  $I_0(\cdot)$  is the modified zeroth-order Bessel function of the first kind and  $Q(\cdot)$  is the Q function. The complex Rice variate was obtained as described in [22]. As in the case of the Nakagami fading case, the validation of the Rice envelope and phase pdfs are shown in Figures 3 and 4, respectively. Notice the close adherence between theoretical and empirical densities.

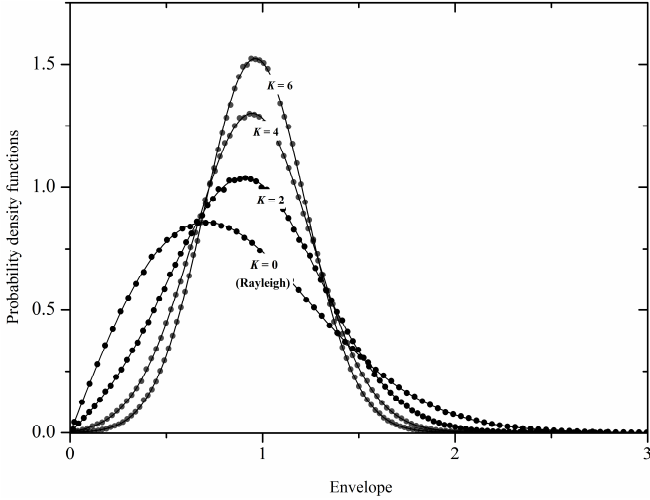


Fig. 3. Empirical and theoretical Rice envelope densities under  $K$  parameter variations

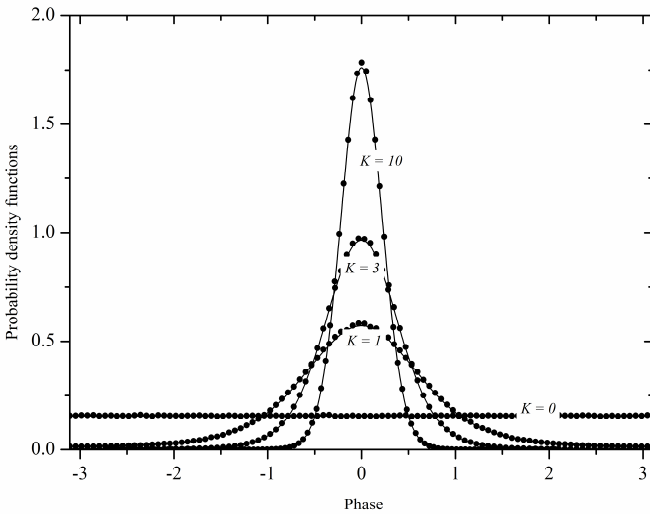


Fig. 4. Empirical and theoretical Rice phase densities under  $K$  parameter variations

### III. SIMULATION RESULTS

This section presents simulation results and discussions concerning the influence of the Nakagami- $m$  and Rice fading parameters on the MED spectrum sensing performance.

A first result to be analyzed shows the variations in the probability of detection of the primary signal,  $P_D$ , with the variations of the signal-to-noise ratio, SNR, of the received

signal. In fading channels, the primary signal captured by a CR suffers from severe fluctuations over time and space because of the behavior of the channel. Under low SNR regime, the detection algorithm should provide high detection probability; otherwise mistakes are made, resulting in missed detections and high interference to the secondary network. Figure 5 shows results of  $P_D$  versus SNR in a multipath Nakagami fading channel, considering  $\ell = 1$  and  $\ell = 6$  cooperating CRs. In each sensing interval, each CR collects  $n = 50$  samples of the primary received signal. The Nakagami phase factor  $p = 0$  maintains a balanced fading model, while the fading factor  $m$  controls the severity of the fading, starting from the more severe condition ( $m = 1$ ), which corresponds to a Rayleigh fading channel, up to the nonfading condition ( $m \rightarrow \infty$ ), which corresponds to a pure AWGN channel. As expected, the influence of increasing the number  $\ell$  of CRs is a performance improvement, considering fixed the remaining parameters. As also expected,  $P_D$  increases as the fading factor  $m$  is increased, for a fixed SNR. This is particularly true in regions of medium to not-very-high values of SNR.

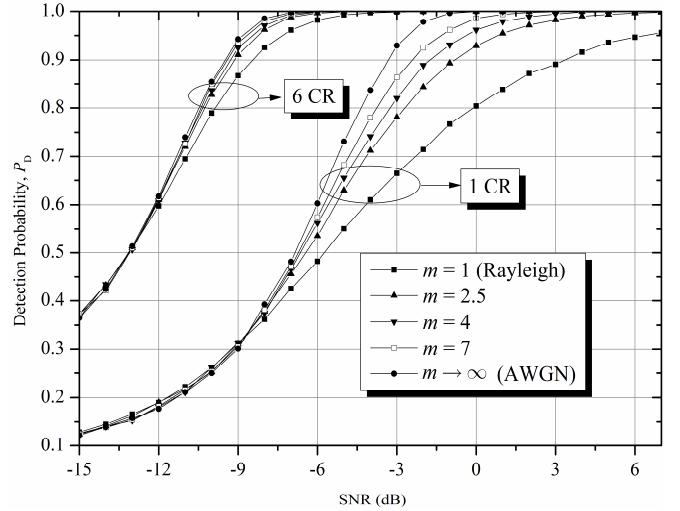


Fig. 5.  $P_D$  versus SNR in a Nakagami- $m$  fading channel

It can also be noticed in Figure 5 that the detection performance improves significantly in the early stages of changes in the fading factor. This is also an expected result, since it is just in these stages that the severity of the Nakagami fading changes in a more pronounced way with changes in  $m$ .

Finally, notice that as  $m \rightarrow \infty$ , the fading effect tends to disappear, which means that the spectrum sensing performance will tend to that produced in a pure AWGN channel.

It is well-known that the Rayleigh multipath fading is characterized by the absence of line-of-sight or any dominant received signal component between transmitter and receiver, whereas the Rice fading is characterized by the presence of such a received signal component of higher intensity. Then, the effect caused by increasing the Nakagami fading factor on the improvement of the detection performance is equivalent as the one caused by increasing the Rice factor. To illustrate this behavior, Figure 6 presents simulation results for the MED

technique using the same settings adopted for constructing Figure 5, except that now a Rice channel is considered, instead of a Nakagami channel.

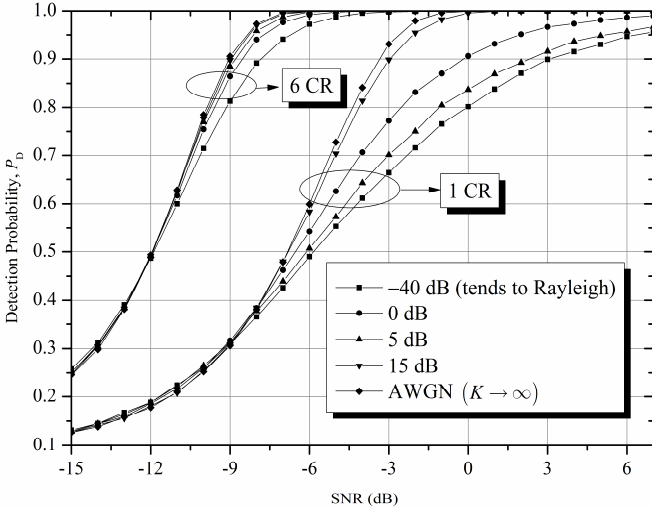


Fig. 6.  $P_D$  versus SNR in a Rice fading channel

From Figure 6 it is evident the improvement in the detection performance due to increased Rice factor, i.e. with increased strength of a LOS or a dominant received signal component, which decreases fading severity. As in the case of the Nakagami fading,  $P_D$  increases in a more pronounced way with an increase in the Rice factor in regions of medium to not-very-high SNR values.

Figure 6 also show extreme-case results: if  $K \rightarrow \infty$ , only a LOS or a single-path received signal component remains, resulting in no fading. In this case the channel becomes a pure AWGN channel. If  $K \rightarrow 0$  ( $-\infty$  dB), the Rice density tends to a Rayleigh density, i.e. the Rice fading turns into a Rayleigh fading, which corresponds to the maximum fading severity. Nevertheless, in [22] it has been pointed out that a Rice factor around  $-40$  dB suffices to produce a fading that very closely match a Rayleigh fading.

Figure 7, which has been constructed considering the absence of primary signal (hypothesis  $\mathcal{H}_0$ ), shows the relationship between the probability of false alarm,  $P_{FA}$ , and the decision threshold  $\gamma$  for different numbers of cooperating CRs in the MED technique. Such results are useful to determine the decision threshold that meets the desired criteria of false alarm rate. It is usual to fix a value for  $P_{FA}$ , a situation known as CFAR (constant false alarm rate), and find the corresponding threshold. As for the previous results, each CR collects  $n = 50$  samples during a sensing interval.

The decision upon the occupation of the sensed channel is arrived by comparing the test statistic given in (3) with decision threshold. A higher threshold maintains the probability of false alarm at low levels, but renders detection difficult. On the other hand, a low threshold favors detection, but increases the false alarm probability. This tradeoff is clearly seen from the receiver operating characteristic (ROC) curve, which shows  $P_{FA}$  versus  $P_D$  as the decision threshold is varied. Figure 8 shows ROC curves for the MED technique on

a Nakagami fading channel, considering a variable fading factor  $m$ ,  $n = 100$  samples per CR, and average SNR =  $-3$  dB. Since the influence of increasing the number  $\ell$  of collected samples per CR is, as expected, a performance improvement considering fixed the remaining system parameters, we consider  $\ell = 1$  CR. Notice that as the fading factor increases, the sensing performance is improved. For example, for a fixed false alarm rate of 0.1, the detection rate goes from around 0.75 in the most severe fading condition ( $m = 1$ ) to approximately 1 in the nonfading condition ( $m \rightarrow \infty$ ).

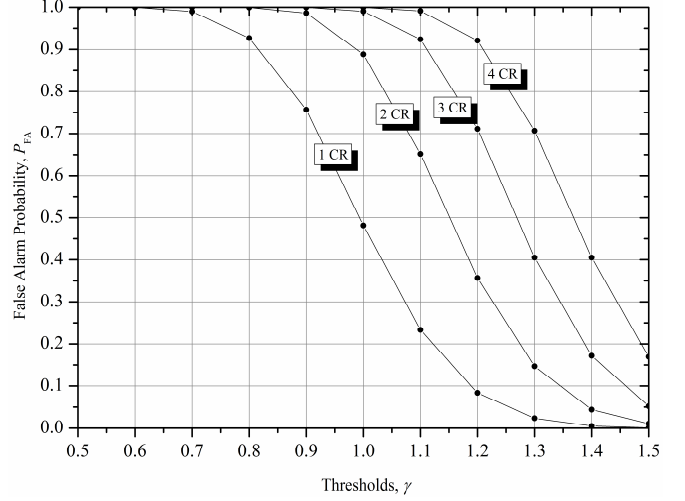


Fig. 7. Performance  $P_{FA}$  versus threshold sensing

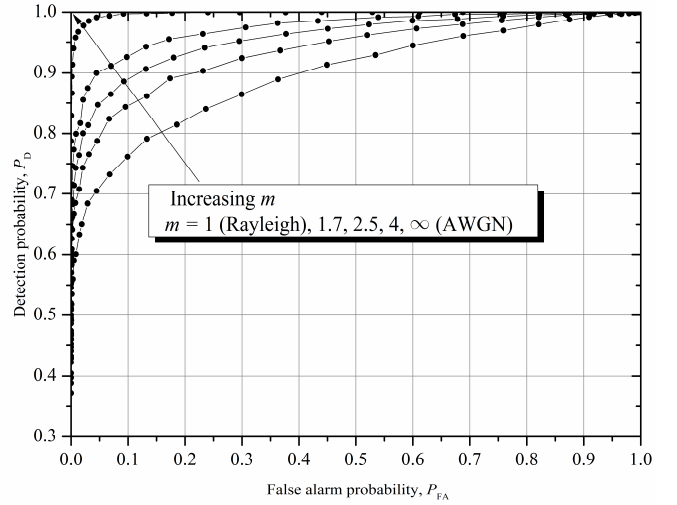


Fig. 8. ROC curves for MED in a Nakagami fading channel

The premise for non-interference in the primary system is a major requirement of opportunistic networks. This makes it desirable to have a low probability of missed detections,  $P_m = 1 - P_D$ , since when a detection is missed the CR network will cause interference to the primary network. Then, another useful curve shows the variations of the miss detection probability and the probability of false alarm, as the decision threshold is varied. This curve is called complementary ROC. Figure 9 shows how  $P_m$  reduces with variations of the Rice factor  $K$  in a Rice fading channel. As expected, the appearance of a LOS or any dominant received signal component brings

reduction in the potential for interference to the primary network since  $P_m$  is reduced. For  $K = 25$  dB, the sensing performance approximates the one obtained in a pure AWGN channel ( $K \rightarrow \infty$ ). As for the case of Figure 8, it has been considered  $\ell = 1$  CR,  $n = 100$  samples per CR, and average SNR =  $-3$  dB.

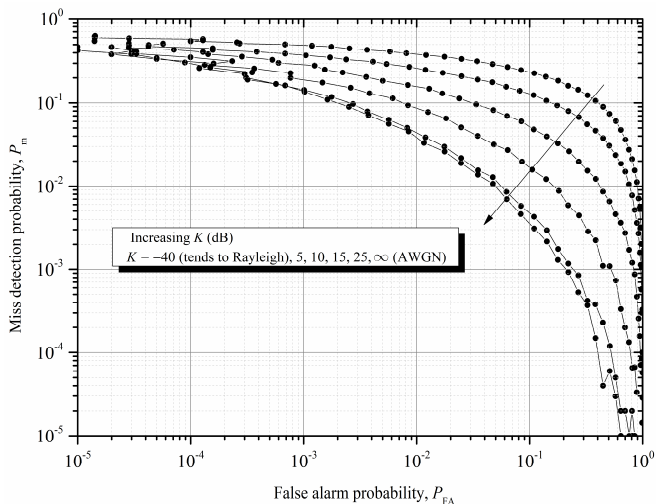


Fig. 9. Complementary ROC curves for MED in a Rice fading channel

#### IV. CONCLUSIONS

This paper presented the results of a performance analysis of the maximum eigenvalue detection (MED) technique applied to the spectrum sensing scenario in Nakagami and Rice fading channels. The analysis unveiled significant variations in the sensing performance in terms of variations in Nakagami fading factor and Rice factor. The modeling of the Nakagami channel reflected envelope and phase statistics, which continue to be an interesting debatable question. It was assumed that the channel conditions were modeled with flat fading. Future studies can evaluate the performance of MED and other sensing techniques in different channel models considering frequency selectivity.

#### V. ACKNOWLEDGMENTS

This project was partially supported by Fapemig under Grant TEC - APQ-01255-12.

#### REFERENCES

- [1] D. Cabric, S.M. Mishra, D. Willkomm, R. Brodersen, and A. Wolisz, "A Cognitive Radio Approach for Usage of Virtual Unlicensed Spectrum," *Proc. 14th IST Mobile and Wireless Comm. Summit*, June 2005.
- [2] J. Mitola III, and G. Q. Maguire Jr., "Cognitive Radio: Making Software Radios More Personal," *IEEE Personal Comm.*, vol. 6, no. 4, pp. 13-18, Aug. 1999.
- [3] I.F. Akyildiz, B.F. Lo, and R. Balakrishnan, "Cooperative Spectrum Sensing in Cognitive Radio Networks: A Survey," *Elsevier Physical Comm.* 4, pp. 40-62, Mar. 2011.
- [4] Y. Zeng, Y.-C. Liang, A. Hoang, and R. Zhang, "A Review on Spectrum Sensing for Cognitive Radio: Challenges and Solutions", *EURASIP Journal on Advances in Signal Processing*, vol. 2010, no 1, p. 381465, 2010.
- [5] T. Yucek and H. Arslan, "A survey of spectrum sensing algorithms for cognitive radio applications," *IEEE Communications Surveys & Tutorials*, vol.11, no.1, pp.116-130, First Quarter 2009.

- [6] A. Kortun, et al., "On the Performance of Eigenvalue-Based Cooperative Spectrum Sensing for Cognitive Radio", *IEEE J. of Selected Topics in Signal Processing*, vol. 5, no. 1, pp. 49-55, Feb. 2011.
- [7] B. Nadler, F. Penna, and R. Garello, "Performance of Eigenvalue-based Signal Detectors with Known and Unknown Noise Level", *Proc. of the IEEE ICC*, Kyoto, Japan, 5-9 Jun. 2011.
- [8] A. Kortun, T. Ratnarajah, and M. Sellathurai, "Exact Performance Analysis of Blindly Combined Energy Detection for Spectrum Sensing", *IEEE PIMRC'10*, 2010.
- [9] S. Ciftci and M.Torlak, "A Comparison of Energy Detectability Models for Spectrum Sensing," *Global Telecommunications Conference, 2008. IEEE GLOBECOM 2008*, pp.1-5, Nov. 30 2008-Dec. 4 2008
- [10] Z. Yonghong, L.Ying-Chang, "Eigenvalue-Based Spectrum Sensing Algorithms for Cognitive Radio" *IEEE transactions on communications*, vol. 57, no. 6, Jun. 2009
- [11] A. Sahai and D. Cabric, "Spectrum sensing: fundamental limits and practical challenges," in *Proc. IEEE International Symp. New Frontiers Dynamic Spectrum Access Networks (DySPAN)*, Baltimore, MD, Nov. 2005.
- [12] D. Cabric, A. Tkachenko, and R. W. Brodersen, "Spectrum sensing measurements of pilot, energy, and collaborative detection," *Proc. Military Commun. Conf. (MILCOM)*, pp. 1-7, Oct. 2006.
- [13] N. Reisi, M. Ahmadian, S. Salari, "Performance Analysis of Energy Detection-based Spectrum Sensing over Fading Channels" *Wireless Communications Networking and Mobile Computing (WiCOM), 2010 6th International Conference on*, pp.1-4, 23-25 Sept. 2010
- [14] M. Nakagami, "The  $m$ -distribution—a general formula of intensity distribution of rapid fading," in *Statistical Methods in Radio Wave Propagation*, W. G. Hoffman, Ed. Oxford, U.K.: Pergamon, 1960, pp. 3-36
- [15] S. O. Rice, *Statistical Properties of Random Noise Currents*, N. Wax, Ed. New York: Dover, 1954, pp. 184-246.
- [16] L. Cheng; B.E. Henty, D.D. Stancil, F. Bai; P. Mudalige.; , "Mobile Vehicle-to-Vehicle Narrow-Band Channel Measurement and Characterization of the 5.9 GHz Dedicated Short Range Communication (DSRC) Frequency Band," *Selected Areas in Communications, IEEE Journal on*, vol.25, no.8, pp.1501-1516, Oct. 2007.
- [17] H. Rasheed and N. Rajatheva, "Spectrum Sensing for Cognitive Vehicular Networks over Composite Fading," *International Journal of Vehicular Technology*, vol. 2011, Article ID 630467, 9 pages, 2011.
- [18] M.D. Yacoub; , "Nakagami- $m$  Phase-Envelope Joint Distribution: A New Model," *Vehicular Technology, IEEE Transactions on*, vol.59, no.3, pp.1552-1557, Mar. 2010
- [19] Q. T. Zhang, "A Decomposition Technique for Efficient Generation of Correlated Nakagami Fading Channels", *IEEE Journal on Selected Areas in Communications*, vol. 18, no. 11, Nov. 2000
- [20] M.D. Yacoub, G. Fraidenraich and J.C.S. Santos Filho, "Nakagami- $m$  phase-envelope joint distribution", *Electron. Lett.* 3rd March 2005 Vol. 41 No. 5
- [21] J. E. Gentle, *Random Number Generation and Monte Carlo Methods*, 2nd edition. Springer, 2005.
- [22] Y. S. Cho, J. Kim, W. Y. Yang, C. G. Kang, MIMO-OFDM Wireless Communications with Matlab, ISBN: 978-0-470-82561-7, - John Wiley & Sons (Asia).